Electronic Supplementary Information: "Linear Response Properties of Solvated Systems: A Computational Study"

Linda Goletto[⊤],[†] Sara Gómez,[‡] Josefine H. Andersen,[¶] Henrik Koch,[*,†,‡] and Tommaso Giovannini[*,‡]

[†]*Department of Chemistry, Norwegian University of Science and Technology, 7491 Trondheim, Norway*

[‡]*Scuola Normale Superiore, Piazza dei Cavalieri 7, 56126 Pisa, Italy*

[¶]*DTU Chemistry–Department of Chemistry, Technical University of Denmark, DK-2800 Kongens Lyngby, Denmark*

E-mail: henrik.koch@sns.it; tommaso.giovannini@sns.it

[⊤] Present address: *Scuola Normale Superiore, Piazza dei Cavalieri 7, I-56126 Pisa, Italy*

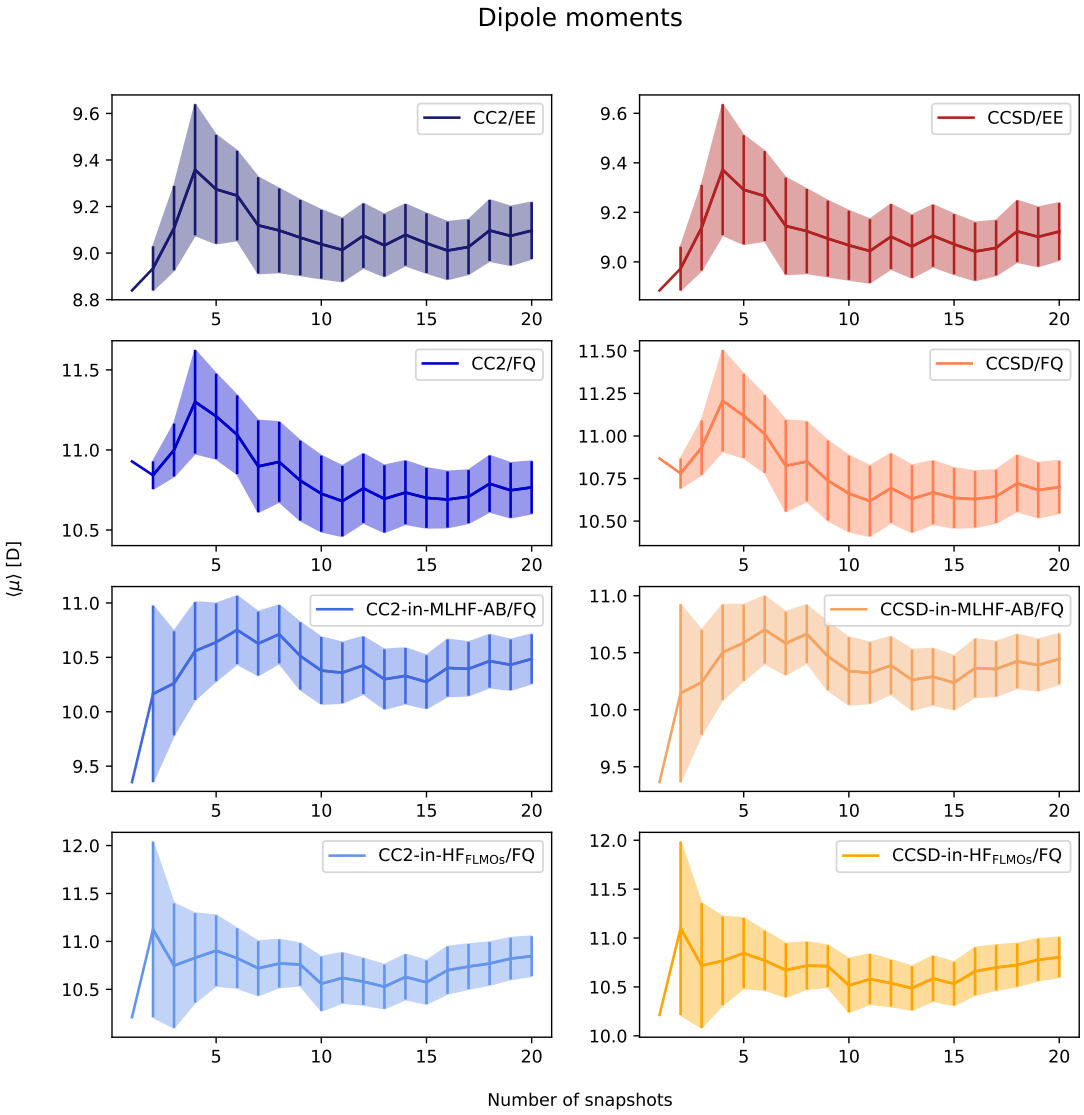

Figure S1: Dipole moment cumulative average of PNA-in-DIO as a function of the number of snapshots. Cumulative standard error bars at the 68% confidence interval are also plotted.

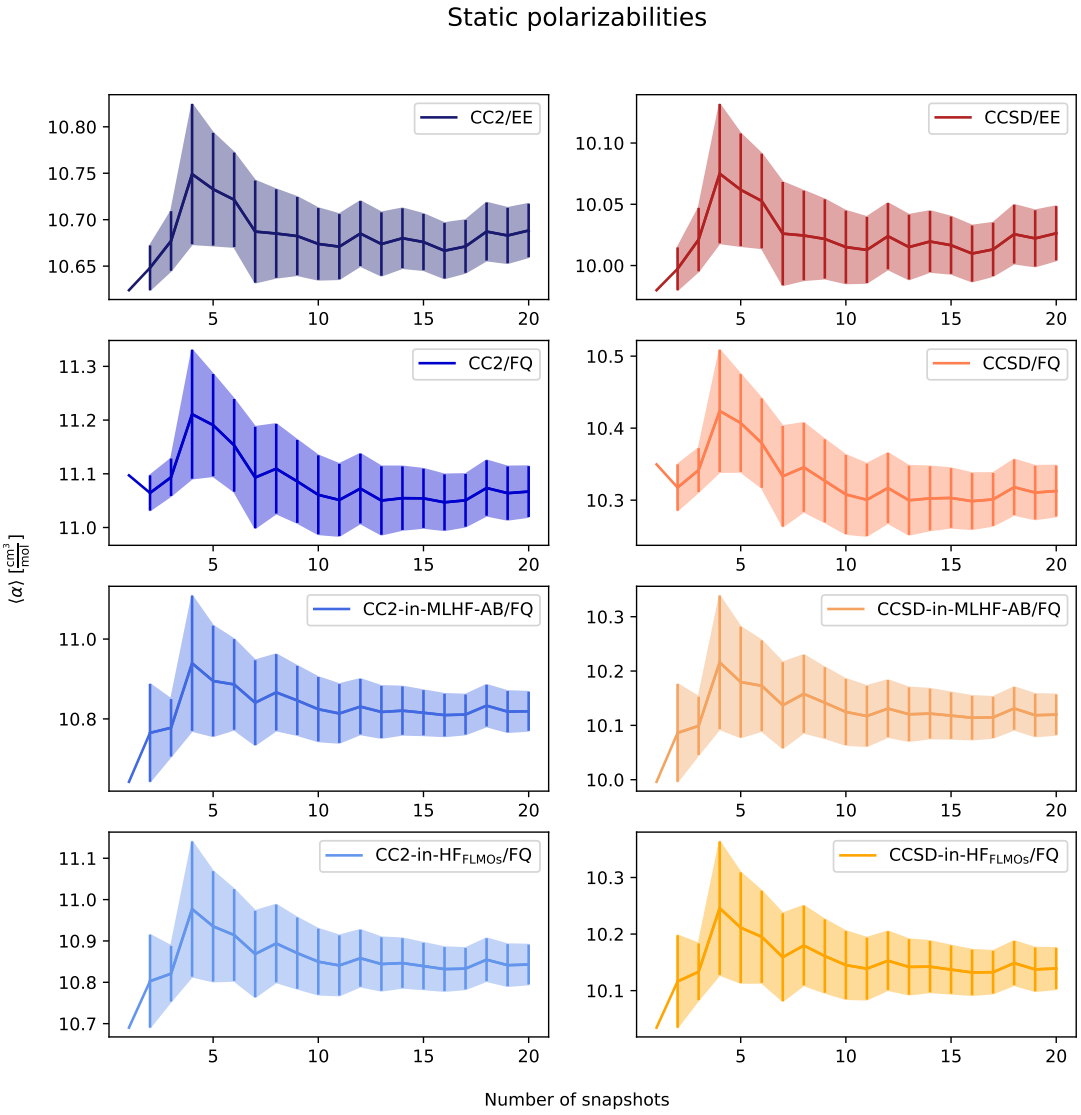

Figure S2: Static electronic polarizability cumulative average of PNA-in-DIO as a function of the number of snapshots. Cumulative standard error bars at the 68% confidence interval are also plotted.

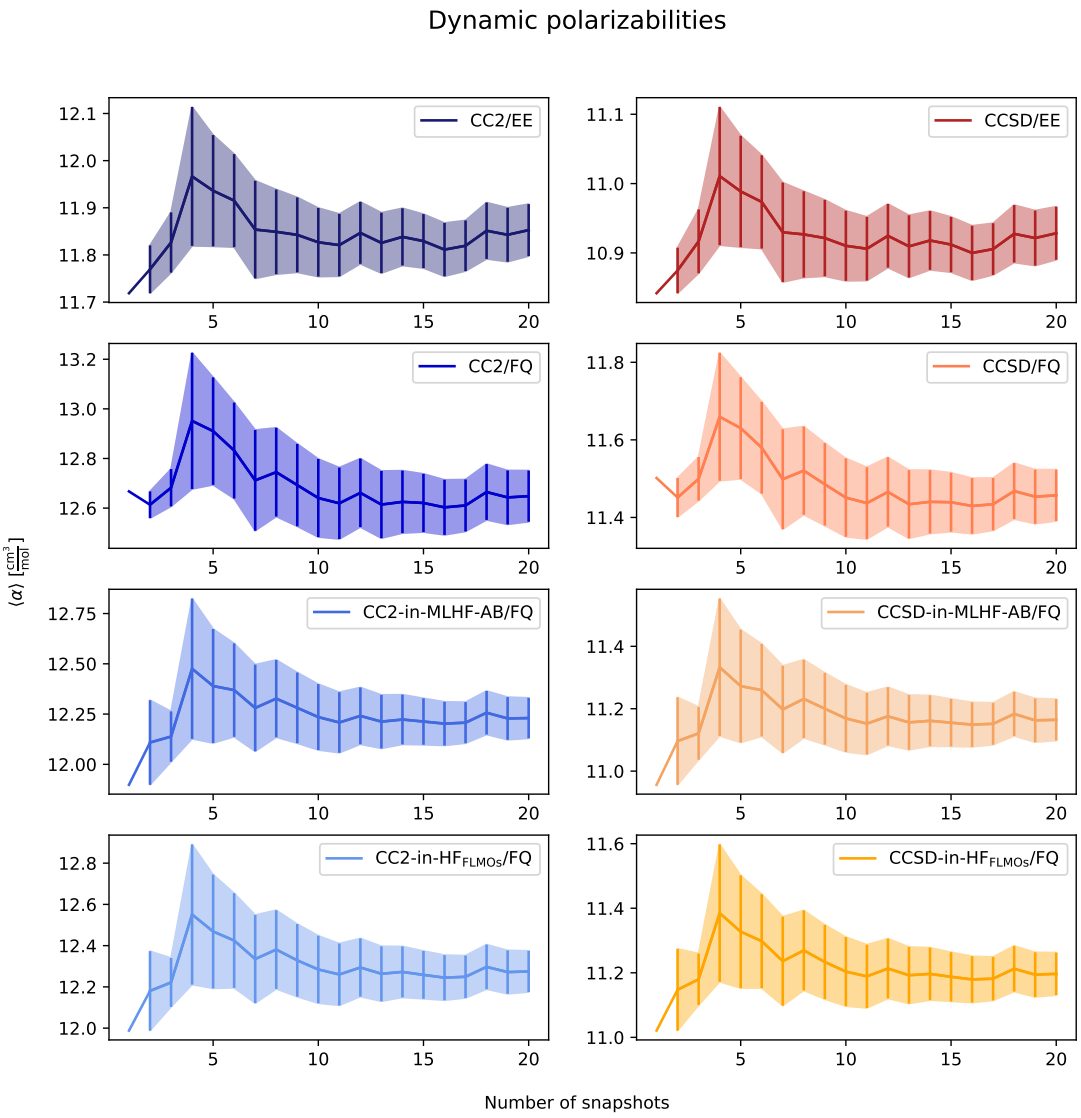

Figure S3: Dynamic electronic polarizability (589 nm) cumulative average for the dynamic electronic of PNA-in-DIO as a function of the number of snapshots. Cumulative standard error bars at the 68% confidence interval are also plotted.

Table S1: Calculated linear polarizabilities at different wavelengths λ of PhCN-in-ACN. The experimental values are reproduced from Ref. 1 ($1\ \frac{\mathrm{cm}^3}{\mathrm{mol}} = 1\ N_A \cdot \mathrm{esu}$, where N_A is the Avogadro constant). [a] employ the Lorentz local field correction, [b] employ the Onsager local field correction.

$\nu[\mu\mathrm{m}^{-1}]$	Method	$\alpha^{\mathrm{iso}}\left[\frac{\mathrm{cm}^3}{\mathrm{mol}}\right]$	Method	$\alpha^{\mathrm{iso}}\left[\frac{\mathrm{cm}^3}{\mathrm{mol}}\right]$	$\alpha^{\mathrm{exp}}\left[\frac{\mathrm{cm}^3}{\mathrm{mol}}\right]$
0.000	CC2 *in vacuo*	8.163	CCSD *in vacuo*	7.832	7.407^a 7.347^b
	CC2/EE	8.201 ± 0.005	CCSD/EE	7.874 ± 0.005	
	CC2/FQ	8.198 ± 0.008	CCSD/FQ	7.874 ± 0.007	
	CC2-in-MLHF-AB/FQ	7.955 ± 0.009	CCSD-in-MLHF-AB/FQ	7.647 ± 0.008	
1.553	CC2 *in vacuo*	8.465	CCSD *in vacuo*	8.102	7.757^a 7.678^b
	CC2/EE	8.511 ± 0.006	CCSD/EE	8.152 ± 0.005	
	CC2/FQ	8.508 ± 0.009	CCSD/FQ	8.152 ± 0.008	
	CC2-in-MLHF-AB/FQ	8.237 ± 0.010	CCSD-in-MLHF-AB/FQ	7.900 ± 0.009	
1.696	CC2 *in vacuo*	8.528	CCSD *in vacuo*	8.158	7.829^a 7.750^b
	CC2/EE	8.576 ± 0.006	CCSD/EE	8.210 ± 0.006	
	CC2/FQ	8.573 ± 0.009	CCSD/FQ	8.210 ± 0.008	
	CC2-in-MLHF-AB/FQ	8.295 ± 0.010	CCSD-in-MLHF-AB/FQ	7.952 ± 0.009	
1.831	CC2 *in vacuo*	8.594	CCSD *in vacuo*	8.216	7.895^a 7.811^b
	CC2/EE	8.643 ± 0.006	CCSD/EE	8.270 ± 0.006	
	CC2/FQ	8.640 ± 0.009	CCSD/FQ	8.270 ± 0.008	
	CC2-in-MLHF-AB/FQ	8.357 ± 0.010	CCSD-in-MLHF-AB/FQ	8.007 ± 0.009	
1.966	CC2 *in vacuo*	8.668	CCSD *in vacuo*	8.282	7.979^a 7.895^b
	CC2/EE	8.719 ± 0.006	CCSD/EE	8.338 ± 0.006	
	CC2/FQ	8.717 ± 0.009	CCSD/FQ	8.338 ± 0.009	
	CC2-in-MLHF-AB/FQ	8.426 ± 0.010	CCSD-in-MLHF-AB/FQ	8.068 ± 0.010	
2.295	CC2 *in vacuo*	8.882	CCSD *in vacuo*	8.471	8.172^a 8.076^b
	CC2/EE	8.939 ± 0.007	CCSD/EE	8.533 ± 0.006	
	CC2/FQ	8.937 ± 0.010	CCSD/FQ	8.534 ± 0.009	
	CC2-in-MLHF-AB/FQ	8.624 ± 0.011	CCSD-in-MLHF-AB/FQ	8.244 ± 0.010	

Table S2: Calculated linear polarizabilities at different wavelengths λ of PhCN-in-THF. The experimental values are reproduced from Ref. 1 ($1\ \frac{\mathrm{cm}^3}{\mathrm{mol}} = 1\ N_A \cdot \mathrm{esu}$, where N_A is the Avogadro constant). [a] employ the Lorentz local field correction, [b] employ the Onsager local field correction.

$\nu[\mu\mathrm{m}^{-1}]$	Method	$\alpha^{\mathrm{iso}}\left[\frac{\mathrm{cm}^3}{\mathrm{mol}}\right]$	Method	$\alpha^{\mathrm{iso}}\left[\frac{\mathrm{cm}^3}{\mathrm{mol}}\right]$	$\alpha^{\mathrm{exp}}\left[\frac{\mathrm{cm}^3}{\mathrm{mol}}\right]$
0.000	CC2 *in vacuo*	8.163	CCSD *in vacuo*	7.832	7.540^a 7.486^b
	CC2/EE	8.190 ± 0.005	CCSD/EE	7.862 ± 0.004	
	CC2/FQ	8.143 ± 0.007	CCSD/FQ	7.822 ± 0.006	
	CC2-in-MLHF-AB/FQ	8.023 ± 0.012	CCSD-in-MLHF-AB/FQ	7.711 ± 0.011	
1.553	CC2 *in vacuo*	8.465	CCSD *in vacuo*	8.102	7.708^a 7.702^b
	CC2/EE	8.499 ± 0.005	CCSD/EE	8.139 ± 0.005	
	CC2/FQ	8.445 ± 0.008	CCSD/FQ	8.095 ± 0.007	
	CC2-in-MLHF-AB/FQ	8.312 ± 0.014	CCSD-in-MLHF-AB/FQ	7.971 ± 0.012	
1.696	CC2 *in vacuo*	8.528	CCSD *in vacuo*	8.158	7.744^a 7.738^b
	CC2/EE	8.563 ± 0.005	CCSD/EE	8.197 ± 0.005	
	CC2/FQ	8.508 ± 0.008	CCSD/FQ	8.151 ± 0.007	
	CC2-in-MLHF-AB/FQ	8.372 ± 0.014	CCSD-in-MLHF-AB/FQ	8.024 ± 0.013	
1.831	CC2 *in vacuo*	8.594	CCSD *in vacuo*	8.216	7.811^a 7.799^b
	CC2/EE	8.631 ± 0.006	CCSD/EE	8.257 ± 0.005	
	CC2/FQ	8.574 ± 0.008	CCSD/FQ	8.210 ± 0.007	
	CC2-in-MLHF-AB/FQ	8.435 ± 0.014	CCSD-in-MLHF-AB/FQ	8.080 ± 0.013	
1.966	CC2 *in vacuo*	8.668	CCSD *in vacuo*	8.282	7.865^a 7.853^b
	CC2/EE	8.707 ± 0.006	CCSD/EE	8.324 ± 0.005	
	CC2/FQ	8.649 ± 0.008	CCSD/FQ	8.276 ± 0.007	
	CC2-in-MLHF-AB/FQ	8.506 ± 0.015	CCSD-in-MLHF-AB/FQ	8.144 ± 0.013	
2.295	CC2 *in vacuo*	8.882	CCSD *in vacuo*	8.471	8.064^a 8.046^b
	CC2/EE	8.926 ± 0.006	CCSD/EE	8.519 ± 0.005	
	CC2/FQ	8.863 ± 0.009	CCSD/FQ	8.467 ± 0.008	
	CC2-in-MLHF-AB/FQ	8.711 ± 0.016	CCSD-in-MLHF-AB/FQ	8.325 ± 0.014	

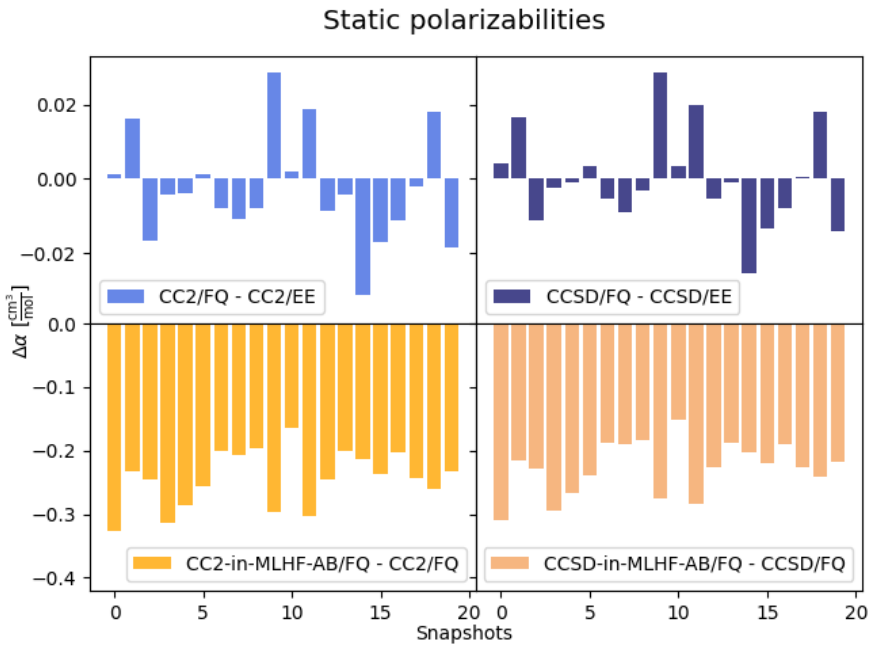

Figure S4: PhCN-in-ACN snapshot-to-snapshot differences between CC-in-MLHF-AB/FQ, CC/FQ, and CC/EE results for the electronic static polarizability.

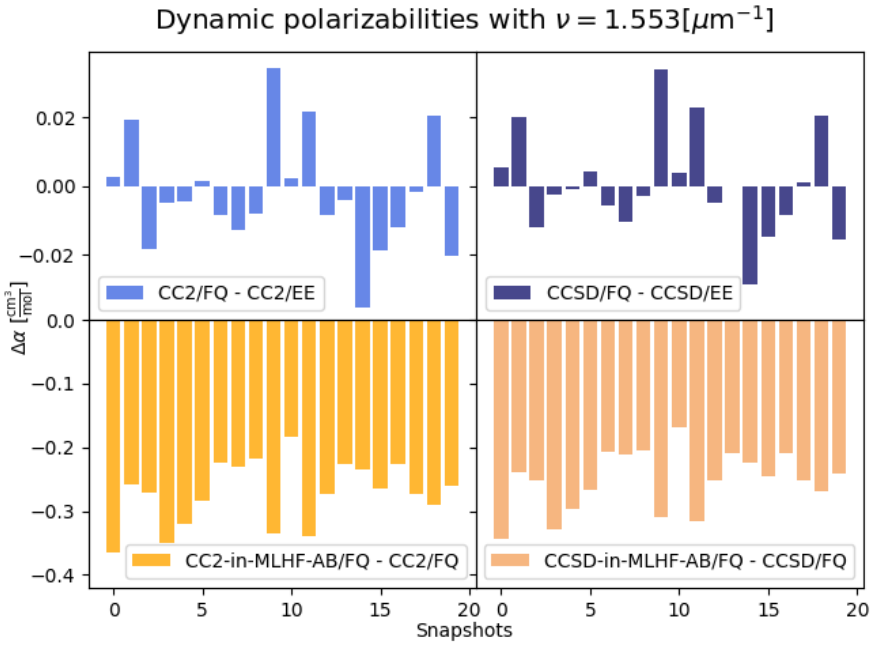

Figure S5: PhCN-in-ACN snapshot-to-snapshot differences between CC-in-MLHF-AB/FQ, CC/FQ, and CC/EE results for the electronic dynamic polarizability, with a frequency of $1.553\,\mu m^{-1}$.

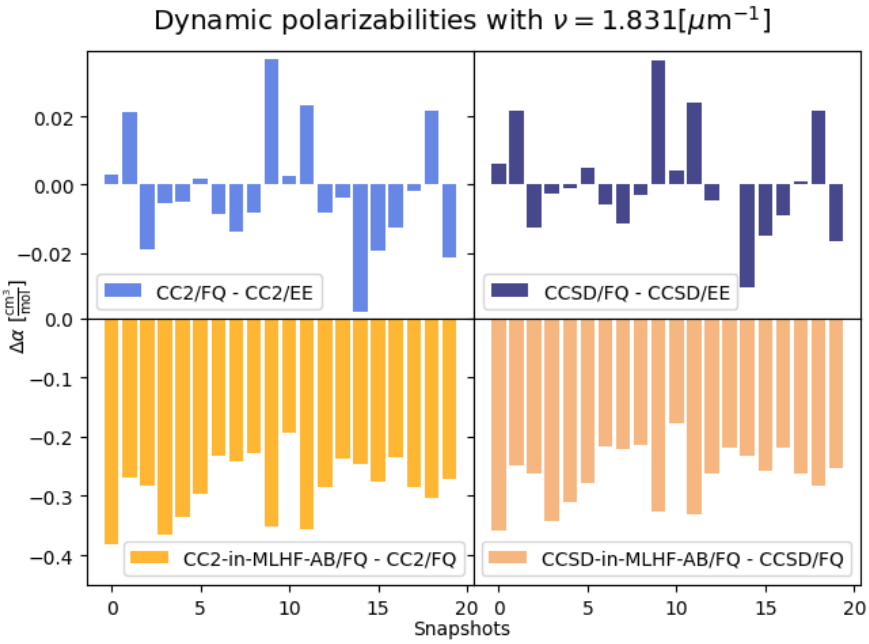

Figure S6: PhCN-in-ACN snapshot-to-snapshot differences between CC-in-MLHF-AB/FQ, CC/FQ, and CC/EE results for the electronic dynamic polarizability, with a frequency of 1.831 µm^{-1}.

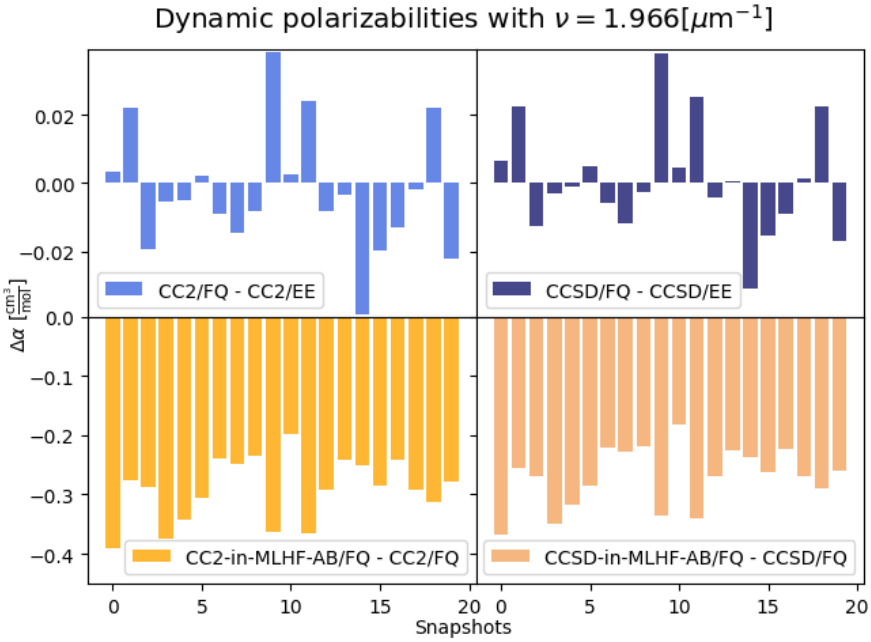

Figure S7: PhCN-in-ACN snapshot-to-snapshot differences between CC-in-MLHF-AB/FQ, CC/FQ, and CC/EE results for the electronic dynamic polarizability, with a frequency of 1.966 µm^{-1}.

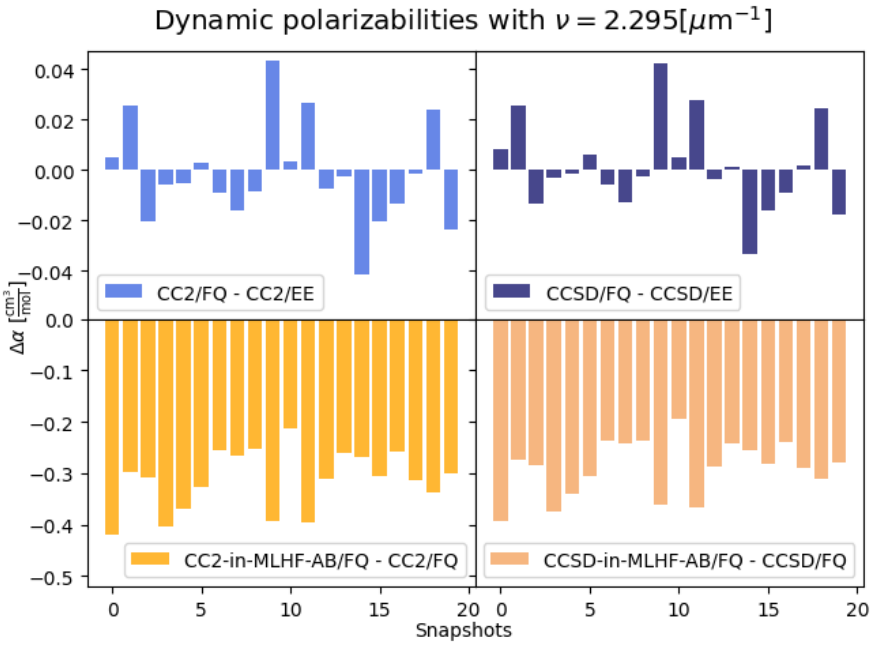

Figure S8: PhCN-in-ACN snapshot-to-snapshot differences between CC-in-MLHF-AB/FQ, CC/FQ, and CC/EE results for the electronic dynamic polarizability, with a frequency of $2.295\,\mu m^{-1}$.

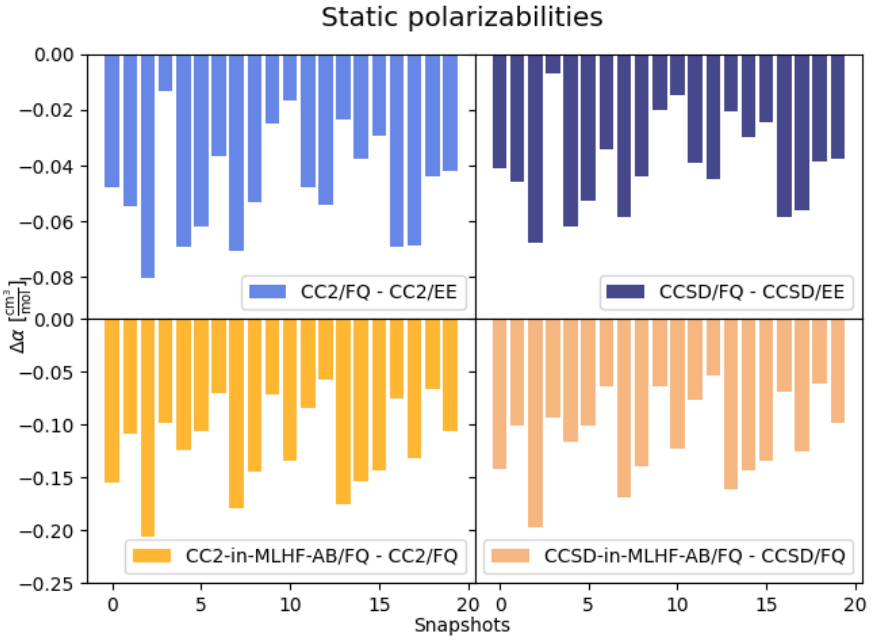

Figure S9: PhCN-in-THF snapshot-to-snapshot differences between CC-in-MLHF-AB/FQ, CC/FQ, and CC/EE results for the electronic static polarizability.

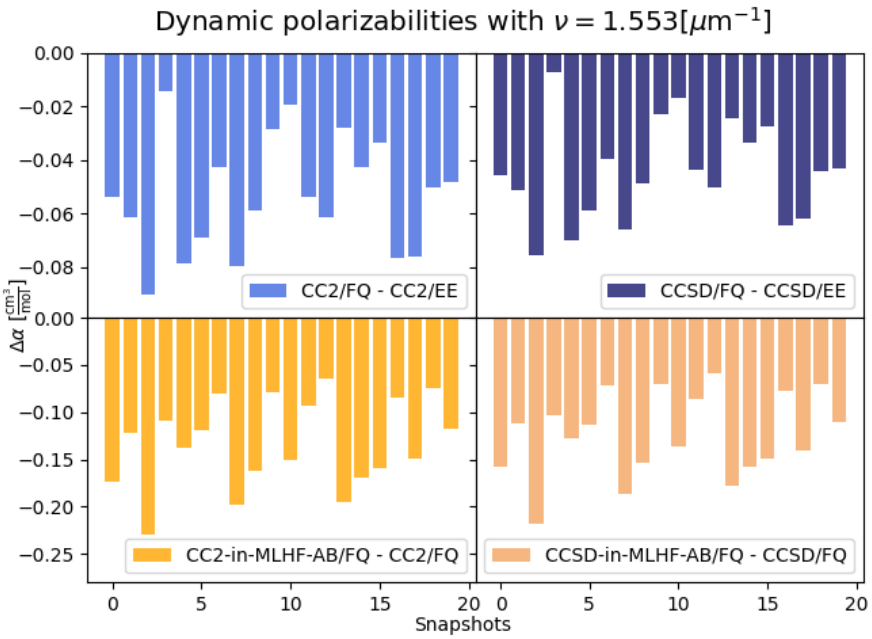

Figure S10: PhCN-in-THF snapshot-to-snapshot differences between CC-in-MLHF-AB/FQ, CC/FQ, and CC/EE results for the electronic dynamic polarizability, with a frequency of 1.553 μm^{-1}.

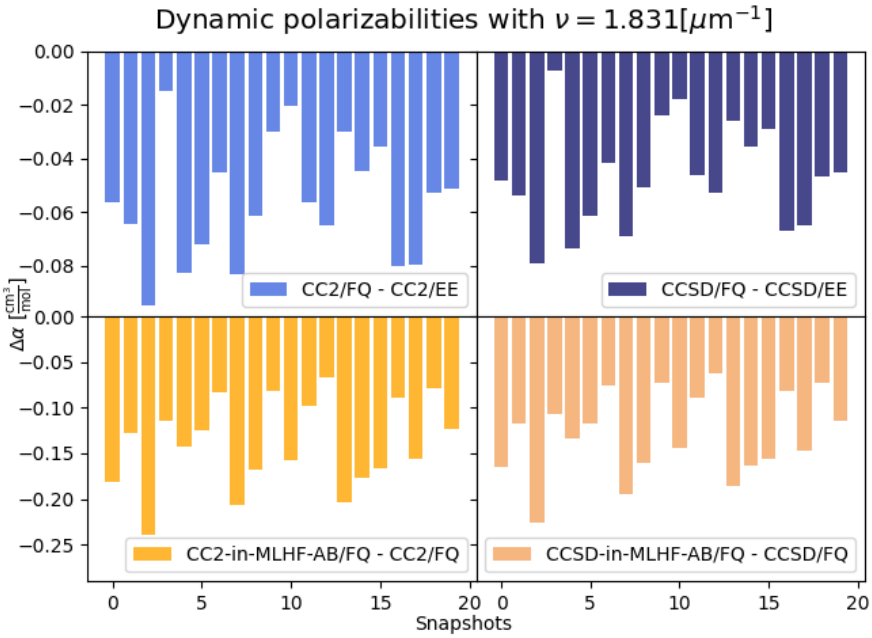

Figure S11: PhCN-in-THF snapshot-to-snapshot differences between CC-in-MLHF-AB/FQ, CC/FQ, and CC/EE results for the electronic dynamic polarizability, with a frequency of 1.831 μm^{-1}.

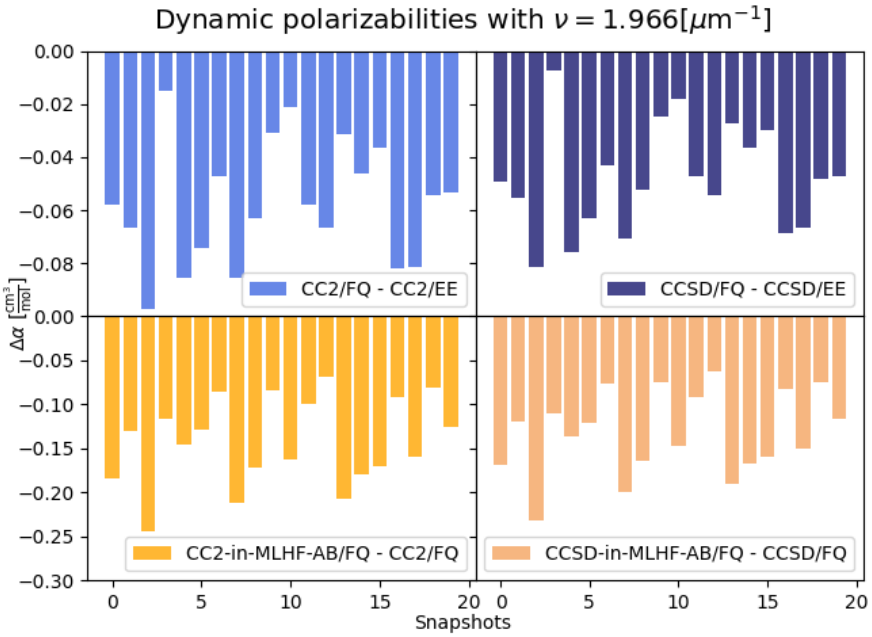

Figure S12: PhCN-in-THF snapshot-to-snapshot differences between CC-in-MLHF-AB/FQ, CC/FQ, and CC/EE results for the electronic dynamic polarizability, with a frequency of 1.966 µm^{-1}.

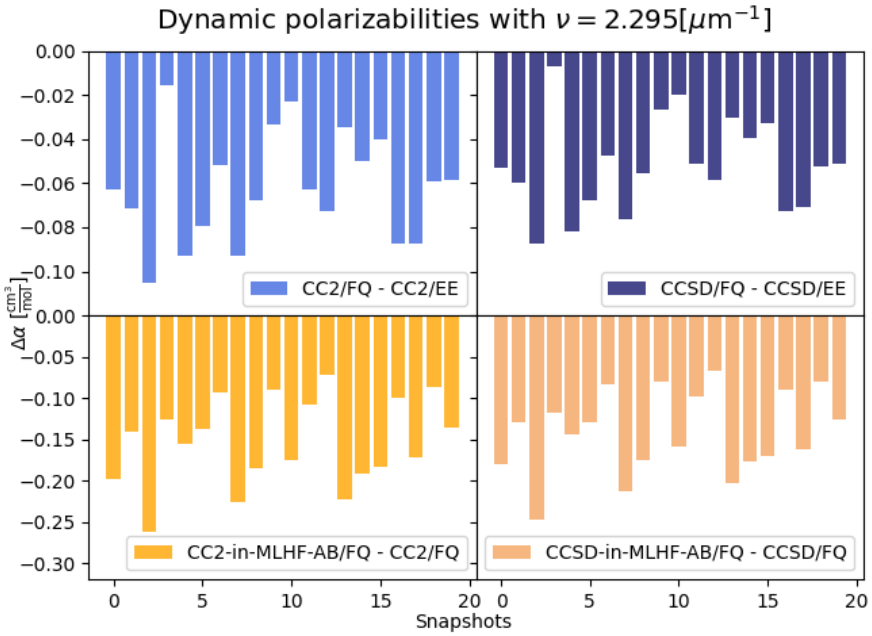

Figure S13: PhCN-in-THF snapshot-to-snapshot differences between CC-in-MLHF-AB/FQ, CC/FQ, and CC/EE results for the electronic dynamic polarizability, with a frequency of 2.295 µm^{-1}.

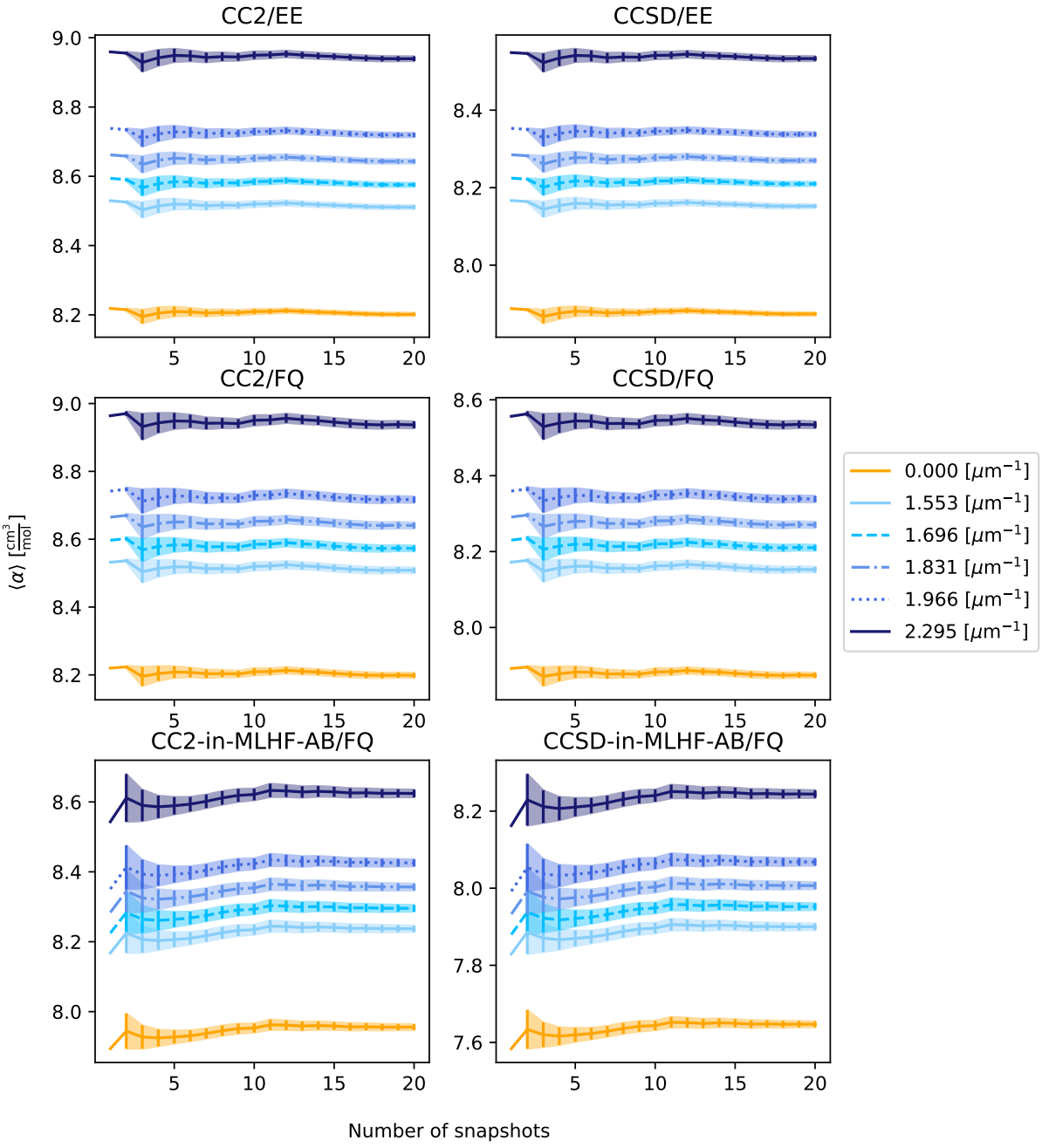

Figure S14: Electronic polarizability cumulative average of PhCN-in-ACN snapshots calculated at different frequencies as a function of the number of snapshots. Cumulative standard error bars at the 68% confidence interval are also plotted.

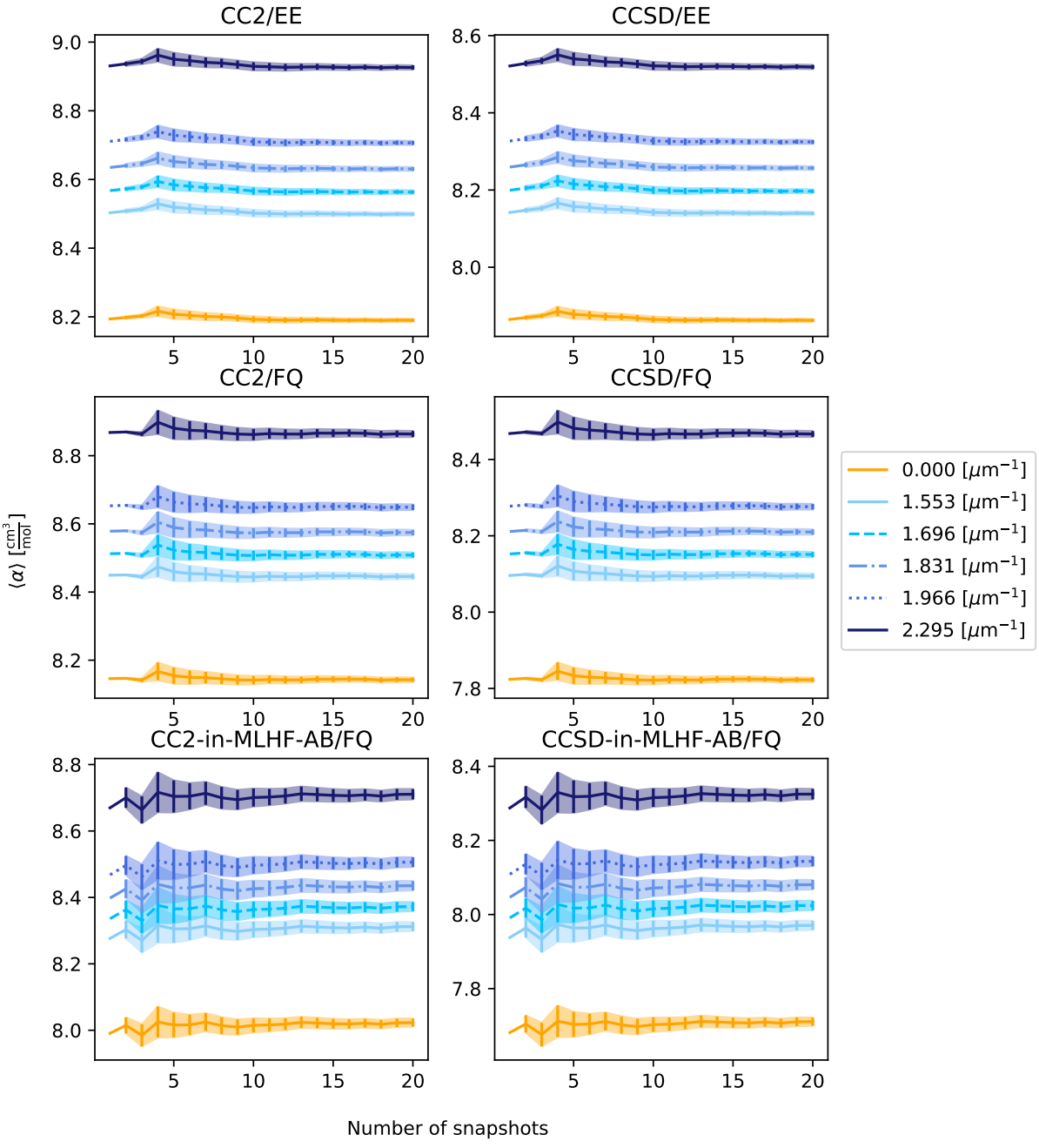

Figure S15: Electronic polarizability cumulative average of PhCN-in-THF snapshots calculated at different frequencies as a function of the number of snapshots. Cumulative standard error bars at the 68% confidence interval are also plotted.

References

(1) Alvarado, Y.; Labarca, P.; Cubillán, N.; Karam, A. Solvent effect on the electronic polarizability of benzonitrile. *Z. Naturforsch. A* **2003**, *58*, 68–74.